

Chemical Ordering of Sputtered FePt / h-BN Granular Media Using RF Substrate Bias

Brandon L. Reese^{1, 2}, Cinthya Aros-Caballero^{1, 2, 3}, Emma Eleson^{1, 2, 4}, Bianca Turner^{1, 5}, B. S. D. Ch. S. Varaprasad^{1, 5}, David E. Laughlin^{1, 2, 5} & Jian-Gang Zhu^{1, 2, 5}

¹Data Storage Systems Center, Carnegie Mellon University, Pittsburgh PA 15213

²Materials Science and Engineering, Carnegie Mellon University, Pittsburgh PA 15213

³Materials Science and Engineering, University of Michigan, Ann Arbor MI 48109

⁴Materials Science and Engineering, Pennsylvania State University, University Park PA 16802

⁵Electrical and Computer Engineering, Carnegie Mellon University, Pittsburgh PA 15213

Abstract

Recently hexagonal-BN (h-BN) / L1₀-FePt granular media has been proposed as an ideal candidate for next generation heat assisted magnetic recording (HAMR) media. The formation of crystalline h-BN at the FePt grain boundaries has resulted in significant enhancements to the sputtered media's microstructural and magnetic properties. While it has been shown that high temperature and RF substrate bias are necessary to achieve highly crystalline h-BN at the grain boundaries, limited discussion has been given to the broader impact of substrate bias on the chemical ordering of FePt within this system. To further evaluate the influence of RF substrate bias on sputtered FePt / h-BN granular media we have prepared several samples using different RF bias powers, 3 W / -21 V_{DC} to 8 W / -70 V_{DC}, on Corning NXTTM glass substrates. It was observed that the L1₀ chemical ordering of the system decreased with increased substrate bias over the above range. This behavior was confirmed in the magnetization data which also reflected a reduction of the out of plane coercivity from 32 kOe to 10 kOe for the -21 V_{DC} and -70 V_{DC} substrate bias samples respectively. Additionally, energy dispersive spectroscopy (EDX) was used to probe the composition of the deposited h-BN / FePt films. This revealed a reduction in the Fe at% observed for all samples deposited with increased substrate bias. Relevant structural, microstructural, magnetic, and compositional data are presented below.

Introduction

Recently the L1₀ FePt / hexagonal-BN (h-BN) system has attracted significant attention regarding its use for heat assisted magnetic recording (HAMR) media [1, 2, 3, 4]. Specifically, this system has yielded significantly improved grain aspect ratios and chemical ordering compared to other systems such as FePt / amorphous carbon (a-C) and FePt / various metal-oxides like TaO_x and SiO_x [5, 6, 7]. Additionally, the large out-of-plane thermal conductivity of h-BN, $k_{h\text{-BN}} = 0.60 \pm 0.05 \text{ W}\cdot\text{m}^{-1}\text{K}^{-1}$, is believed to reduce down track thermal gradients in HAMR media, a key factor regarding improved bit density [4]. While the FePt / h-BN system promises many enhancements over current HAMR media technologies, limited discussion has been given to its behavior on conventional glass substrates [2, 8]. Much of the pioneering work performed on FePt / h-BN investigated its behavior using doped Si substrates [1, 3, 4]. As discussed by C. Xu et al. the key to achieving FePt / h-BN granular media relies on the crystallization of BN into the hexagonal phase. To crystallize sputtered BN two conditions are generally required, high temperature, $T > 500 \text{ C}$, and a small substrate bias, typically $V_{DC} \sim -15 \text{ V}$ [1].

Therefore, when transitioning to glass substrates it is expected that the self-biasing behavior associated with an RF substrate bias will change the conditions necessary to achieve highly ordered and well crystallized L1₀ FePt / h-BN granular media.

Additionally, we discuss the role of the RF substrate bias as it may relate to reverse sputtering processes. The threshold energies and experimental sputter yields of Fe and Pt atoms are 20 eV / 3.4 atoms per ion and 25 eV / 3.0 atoms per ion respectively [9, 10]. This suggests that Fe atoms preferentially reverse sputter from the film surface near the voltages used to produce FePt / h-BN granular media. This results in films that are Pt rich. Pt enrichment of the deposited media may explain the reduced ordering seen for increased bias voltages within the FePt / C-BN system [8].

Therefore, the presence of an RF substrate bias modifies the local chemistry of FePt thin films resulting in reduced chemical ordering.

To further evaluate this claim, we present an experimental study investigating the chemical ordering of FePt / h-BN granular media deposited using different RF substrate bias voltages.

Samples were prepared at high temperature using magnetron sputtering and their magnetic, structural, and chemical properties were evaluated using various experimental techniques outlined below. It was found that samples deposited using low bias voltages, $V_{DC} \sim -21$ V, resulted in good $L1_0$ chemical ordering and magnetic properties. However, as the bias voltage was increased the measured Fe content in the films decreased significantly leading to the appearance of an $L1_2$ $FePt_3$ phase.

Methods

Media samples of BN | FePt were sputtered onto a layered stack of MgO (8nm) | Cr (30nm) | a-Ta (5-10nm) | glass substrate using an AJA sputtering system, base pressure 1×10^{-8} Torr. All sputtering targets were composed of material of 3N purity or higher. For the media layer, composite targets, FePt (Fe 55 at% / Pt 45 at%) and BN (B 50 at% / N 50 at%), were co-sputtered to form the desired films.

To form the necessary underlayers Ta was first deposited at room temperature onto Corning NXTTM glass substrates. The Ta surface was then exposed to O_2 atmosphere (0.1 mTorr) for 1 minute to help form (002) texture in the following Cr layer. Next, a 30 nm thick Cr layer was deposited at 280 °C to achieve a good (002) texture. To reduce surface roughness and attain large Cr grain sizes, the samples were then annealed at 700 °C for 1 hr. An 8 nm MgO layer was finally deposited at room temperature. The distance between targets and the substrate were roughly 80mm.

For the following media layers samples were preheated to $T = 650$ °C for 30 minutes before FePt and BN were co-sputtered using 6 mTorr of Ar. To start, a nucleation layer of 0.5 nm FePt was sputtered onto the MgO underlayer followed by 1 nm FePt (20W DC) + 34 vol% amorphous-BN (a-BN) (190W RF). The nucleation layer and 1nm FePt + a-BN remained the same for all 6 samples.

After the nucleation and coarsening stage described above, substrate biases were applied to the samples. The FePt target power was adjusted to achieve roughly the same BN fractions for all samples. Six samples using powers of 3 W to 8 W RF substrate bias were prepared, this

corresponded to DC voltages of -21 V_{DC} to -70 V_{DC}. To maintain the correct BN fractions deposition times were increased from ~ 7 mins (-21 V_{DC}) to ~ 8.5 mins (-70 V_{DC}). As outlined by C. Xu et al. the temperature and BN fraction within the film was gradually decreased. The temperature reduction helps annealing artifacts observed in thicker media. For reference, C. Xu's 16 nm media required $\sim 11 - 13$ mins to complete the media layer [3]. Noting that prior reports on thinner media, 11.5 nm [1], did not require a thermal gradient we decided to implement a 25 °C gradient in our samples. The final step in our process decreased temperature from $T = 650$ °C / 28 vol% (4.5 nm) BN + RF bias to $T = 625$ °C / 24 vol% (7 nm) BN + RF bias resulting in a total film thickness of ~ 13 nm.

Standard X-ray diffraction (XRD) with a Cu-K α source was used to characterize the texture and ordering of all samples. The microstructure of the samples was evaluated using scanning transmission electron microscopy (STEM) and high-resolution electron microscopy (HRTEM). High angle annular dark field (STEM-HAADF) images are provided. All STEM data presented were collected using an FEI Titan Themis 200 while HRTEM data was collected on an FEI Tecnai F20. Compositional analysis was performed inside the STEM using a Thermo Fisher super-x energy dispersive spectroscopy (EDX) detector. Room temperature magnetic field measurements were performed using a Quantum Design Magnetic Property Measurement System (MPMS) with attached Vibrating Sample Magnetometer (VSM).

Results and Discussion

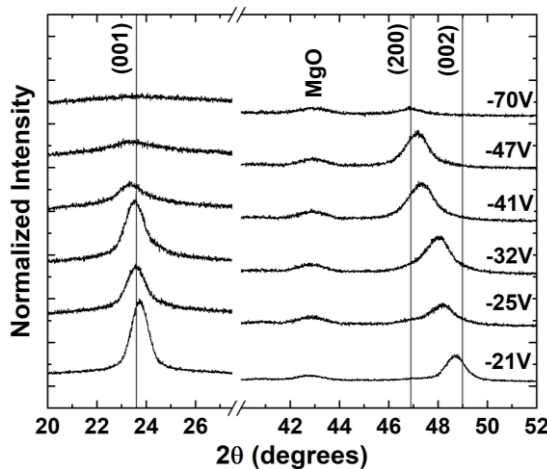


Fig. 1: XRD for samples deposited using marked RF substrate bias voltages.

Several samples of granular media containing approximately 28 - 24 vol% h-BN were deposited at different substrate bias powers. The corresponding XRD data is provided in **Fig. 1**. As shown, the (001) superlattice reflection of $L1_0$ -FePt disappears and the ordered (002) peak shifts toward the disordered (200) peak with increased substrate bias voltage. The degradation of FePt ordering with increased bias voltages occurs monotonously. At lower voltages, -21 V_{DC} and -25 V_{DC} , a small (200) shoulder could also be observed suggesting a small fraction of either in-plane $L1_0$ or disordered FePt. As the bias voltage increased further, the diffracted intensities decreased significantly, suggesting a loss of (001) texture.

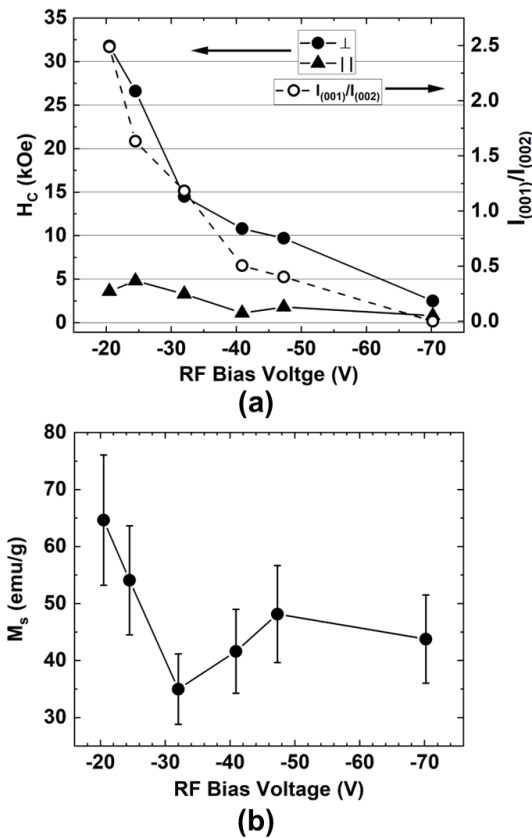


Fig. 2: In-plane / out-of-plane coercive fields and integrated intensity ratios, $I_{(001)}/I_{(002)}$, for the $L1_0$ -FePt XRD peaks plotted as a function of applied substrate self-bias voltages (a). Saturation magnetization given as a function of substrate self-bias voltages (b).

Room temperature in-plane and out-of-plane magnetization measurements have also been performed which confirmed a reduction of $L1_0$ ordering for increased bias voltages, see **Fig. 2**. Intensity ratios for the (001) and (002) type diffraction peaks are also provided in the figure. For reference, the ratio, $I_{(001)}/I_{(002)}$, of integrated intensities for fully ordered $L1_0$ FePt should be ~ 4 [11]. As shown, $I_{(001)}/I_{(002)}$ decreases from ~ 2.5 to ~ 0.4 for the samples deposited at RF bias

voltages of -21 V_{DC} and -47 V_{DC} respectively. No superlattice peak was observed for the sample deposited using -70 V_{DC} substrate bias. With decreased intensity ratios, the in-plane coercivity of the samples remained relatively constant for all bias voltages, $H_C < 5$ kOe. The out-of-plane component decreased from $H_C = 31.8$ kOe to $H_C = 2.4$ kOe, roughly following the same trend observed in the diffraction data. This behavior further confirms that the deposited films exhibited reduced L₁ ordering for increased bias voltages. Comparing again with **Fig. 1**, it is also apparent that increased RF bias voltage results in both poor texture and limited L₁ ordering.

Calculations to determine the saturation magnetization (M_S) of the samples were also performed, see **Fig. 2** (b). The results presented here assumed an error of 500 μm when cleaving the square specimens for magnetic characterization. The relative volume fraction of FePt to BN was determined via analysis of plane-view STEM-HAADF images. As shown in **Fig. 3 (a and c)**, the relative vol% of FePt grains changed significantly from ~ 60 vol% to ~ 50 vol% for the -21 V_{DC} and -70 V_{DC} samples respectively. The density of FePt was taken to be 14.98 g/cm³ so that a mass could be associated with each sample. As shown, the results for low bias samples match well with existing literature regarding the saturation moment of ordered FePt [12]. Notably, a small recovery in M_S is observed from ~ 35 emu/g to ~ 48 emu/g for the -32 V_{DC} and -47 V_{DC} samples respectively. This trend does not match with the measured ordering and coercivities shown in **Fig. 1 (a)**.

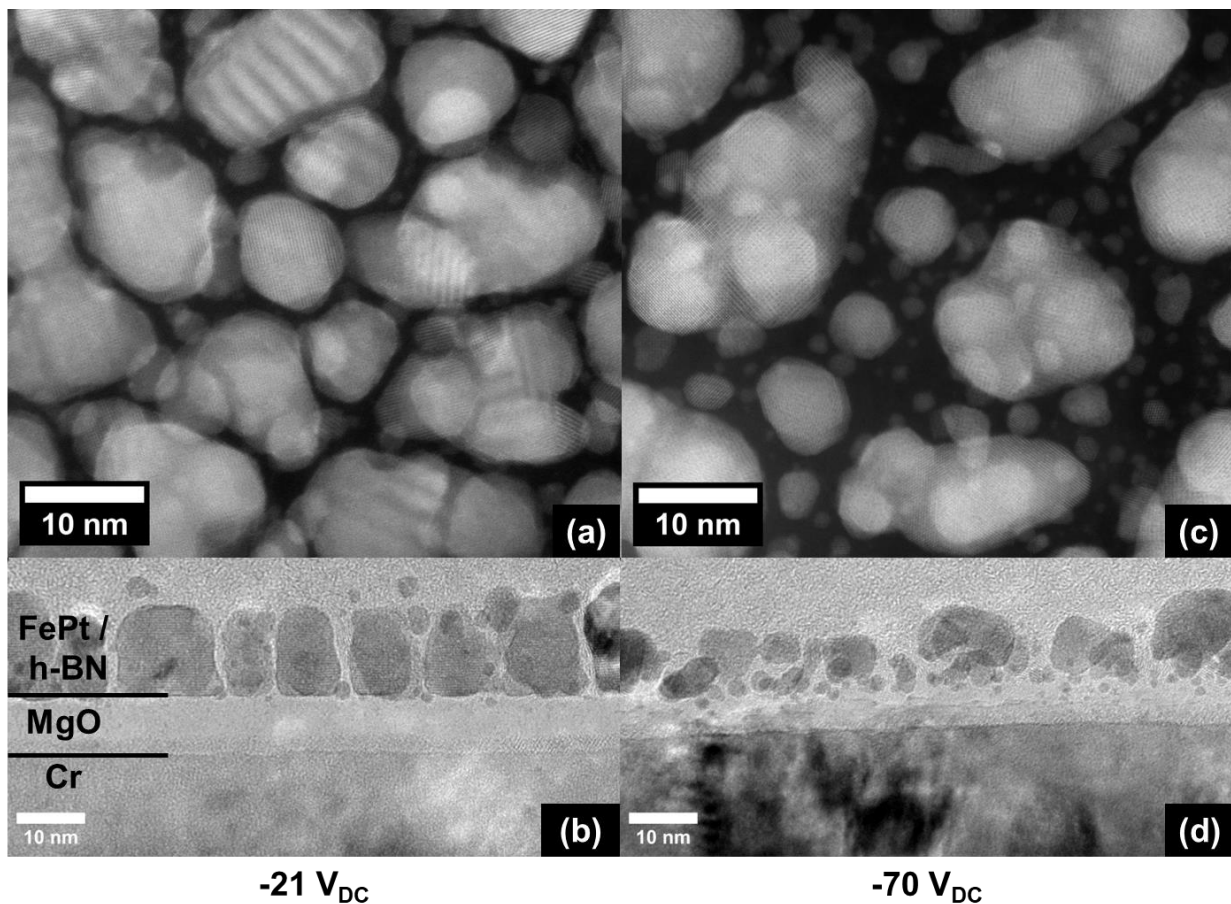


Fig. 3: Plane-view STEM-HAADF and corresponding HRTEM cross-sections for the samples deposited using -21 V_{DC} (a and b) and -70 V_{DC} (c and d). Labels for Cr, MgO, and FePt / h-BN layers are representative for both (b) and (d) HRTEM images.

To further probe the ordering and texture of films deposited using large bias voltages, a TEM survey was performed. **Fig. 3 (a and c)** shows plane-view STEM-HAADF images of the -21 V_{DC} and -70 V_{DC} samples respectively. With increased bias potential the FePt grain structure tends toward large distant grains separated by many smaller grains with wide grain boundaries. As mentioned, the amount of FePt decreased roughly 10 vol% from 60 vol% (-21 V_{DC}) to 50 vol% (-70 V_{DC}). To further confirm the loss of texture discussed above cross-sections for the samples deposited using -21 V_{DC} and -70 V_{DC} substrate bias are provided, see **Fig. 3 (b and d)**. At elevated bias conditions, $V_{DC} < -41$ V, the MgO layer is etched away. This degrades the (001) texture of the samples. The thickness of the MgO layer reduced from ~ 8 nm to ~ 5 nm for the -21 V_{DC} and -70 V_{DC} samples respectively. Here, it should be noted that the process for all films was identical up to the FePt / a-BN coarsening step, any change in the MgO layer or FePt microstructure can be attributed to the applied bias. At lower bias settings, -21 V_{DC} shown in **Fig. 3 (b)**, the samples are

single layer and show a well isolated grain structure. This behavior is consistent with the XRD data which showed a significant decrease in the diffracted intensities for elevated bias settings.

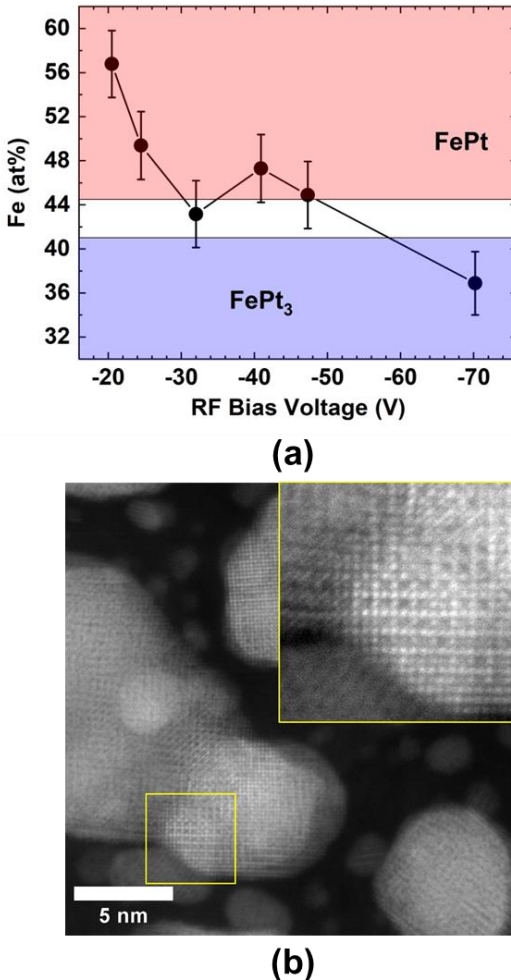


Fig. 4: Fe content within the deposited films as determined via EDX taken across a $3\mu\text{m} \times 3\mu\text{m}$ field of view. Relevant equilibrium phases are provided in the figure, FePt (red) and FePt₃ (blue) (a). STEM-HAADF showing the existence of an L1₂ FePt₃ phase in the film deposited using -70 V_{DC} RF substrate bias (b).

Additional EDX measurements were conducted to characterize the Fe / Pt content of all samples. Spectra obtained over a $3\mu\text{m} \times 3\mu\text{m}$ field of view of the granular films were analyzed using a Cliff-Lorimer method. Stock k-factors, provided within Velox software, of $K_{\text{Fe}} = 1.00$ and $K_{\text{Pt}} = 1.76$ for the Fe-K α and Pt-L α peak were used to compute relative Fe/Pt concentrations. Additional calculations for Fe/Pt content were performed using the k-factor $K_{\text{PtFe}} = I_{\text{Fe}}/I_{\text{Pt}} = 0.80 \pm 0.02$ cited by [13, 14], however, these measurements appeared to overestimate the Fe content of the deposited films; the sputtering target used in these experiments contained just 55 at% Fe. **Fig. 4 (a)** shows that the observed Fe content in the deposited media decreases significantly at increased bias

voltages with a small recovery near the -41 V_{DC} sample. At sufficiently high bias voltages the equilibrium microstructure could exist as a mixture of FePt-FePt₃, or in the case of the sample deposited using -70 V_{DC} bias, be largely FePt₃. The STEM high angle annular dark field (STEM-HAADF) image provided in **Fig. 4 (b)** shows a region of the -70 V_{DC} sample that has ordered to the L1₂ FePt₃ phase, confirming that higher bias voltages result in reduced Fe content [14].

The reduction of Fe content for increased bias voltage is likely associated with the different threshold energies of Fe and Pt atoms in the deposited film. The threshold energies of either atom for incident Ar ions are 20 eV and 25 eV respectively [9]. Since the FePt layer is sufficiently thin there is no depth at the film surface to accommodate the different sputter yields of either atom, 3.4 and 3.0 atoms per incident ion for Fe and Pt respectively [10]. As a result, the weakly bound Fe atoms are preferential reverse sputtered leaving behind a grain structure that is largely Pt rich, a trend also observed for similar Cu-Pt and Ni-Pt systems [10]. Interestingly, the small recovery in Fe at% seen at -41 V_{DC} likely indicates that the Pt threshold voltage of this system has been reached. Beyond ~ -35 to -40 V_{DC} substrate bias the Pt also begins to experience the reverse sputtering effect and both atoms are removed from the film surface. This results in the small recovery in Fe at% seen for the sample deposited using -41 V_{DC} substrate bias, see **Fig. 4 (a)**. As further confirmation of this effect, a similar recovery in M_S at -41 V_{DC} can also be observed in **Fig. 2 (b)**.

Interestingly, the onset of Pt reverse sputtering appears to be coupled with the degraded microstructure shown in **Fig. 3 (d)**. This suggests that at sufficiently low bias voltages the Pt atoms that remain within the grains preserve the microstructure of the deposited films. Once Pt atoms begin to reverse sputter from the deposited film the microstructure reorganizes, likely to due to a redeposition process, into the disordered microstructure shown in **Fig. 3 (d)**. This indicates that there is a very small region, roughly -21 V_{DC} to -40 V_{DC}, where the composition and ordering of deposited films can be controlled via RF bias without destroying the microstructure / texture of the deposited films.

Conclusion

We have observed a reduction in Fe content within FePt / h-BN granular media for increased RF substrate bias voltages over the optimal condition. The reduction of Fe content within the films resulted in decreased $L1_0$ ordering and degraded magnetic properties. This effect can be attributed to slightly different threshold binding energies of either Fe or Pt atoms within this system. At low bias voltages the Fe is preferentially reverse sputtered away from the film surface resulting in Pt rich media with good texture and microstructure. Once a threshold voltage of roughly -41 V_{DC} is reached both atoms are reverse sputtered from the film surface. The resulting texture and microstructure of the media degrades significantly with further increase to the applied substrate bias. At sufficiently high bias voltages, $V_{DC} \sim -70$ V, an $L1_2$ FePt₃ phase appears. The existence of FePt₃ serves as further evidence that substrate bias preferentially targets Fe atoms. In general, we find that an Fe deficiency within the deposited media can be controlled in-situ using RF substrate bias. The reduced Fe content within the FePt media has resulted in the loss of $L1_0$ ordering. Although $L1_0$ ordering degrades for low bias voltages, significant changes to the film microstructure are not observed until the threshold voltage for Pt atoms has been reached and both atoms reverse sputter from the film surface.

Acknowledgement

This research was funded by the Data Storage Systems Center at Carnegie Mellon University and all its industrial sponsors and by the Kavcic–Moura Fund at Carnegie Mellon University. Emma Eleson and Cynthia Aros-Caballero were supported by an NSF-REU site award (DMR-2244316) as part of a collaboration with the Semiconductor Research Corporation (SRC). The authors acknowledge the use of the Materials Characterization Facility at Carnegie Mellon University supported by Grant No. MCF-677785.

References

¹ C. Xu, B. S. D. Ch. S. Varaprasad, D. E. Laughlin, and J.-G. Zhu, "Bias sputtering of granular L₁₀-FePt films with hexagonal boron nitride grain boundaries," *Sci. Rep.*, vol. 13, no. 11087, 2023. doi: 10.1038/s41598-023-38106-9

² B. S. D. Ch. S. Varaprasad, C. Xu, M.-H. Huang, D. E. Laughlin, and J.-G. Zhu, "FePt–BN granular HAMR media with high grain aspect ratio and high L₁₀ ordering on corning LotusTM NXT glass," *AIP Adv.*, vol 13, no. 3, pp. 035002, 2023. doi: 10.1063/9.0000587

³ C. Xu, B. S. D. Ch. S. Varaprasad, D. E. Laughlin, J.-G. Zhu, "Fabrication of 16 nm Thick Granular L₁₀ FePt-*h*BN Thin Film Media," *IEEE Trans. Magn.*, vol. 59, no. 11, 2023. doi: 10.1109/TMAG.2023.3294354

⁴ C. Xu, E. Zhang, B.-Y. Yang, B. S. D. Ch. S. Varaprasad, D. E. Laughlin, and J.-G. Zhu, "Thermal Conductance Analysis of the [FePt/h-BN/FePt] Interface," *IEEE Trans. Magn.*, 2024. doi: 10.1109/TMAG.2024.3480129

⁵ P. Tozman, S. Isogami, I. Suzuki, A. Bolyachkin, H. Sepehri-Amin, S. J. Greaves, H. Suto, Y. Sasaki, T. Y. Chang, Y. Kubota, P. Steiner, P.W. Huang, K. Hono, and Y. K. Takahashi, "Dual-layer FePt-C granular media for multi-level heat-assisted magnetic recording," *Acta Mater.*, vol. 271, pp. 119869, 2024. doi: 10.1016/j.actamat.2024.119869

⁶ I. Suzuki, H. Sepehri-Amin, K. Hono, and Y. K. Takahashi, "Control of grain density by varying lattice mismatch in FePt-C film for heat assisted magnetic recording," *J. Alloys Compd.*, vol. 968, pp. 172196, 2023. doi: 10.1016/j.jallcom.2023.172196

⁷ S. D. Granz, K. Barmak, and M Kryder, "Granular L₁₀ FePt:X (X = Ag, B, C, SiO_x, TaO_x) thin films for heat assisted magnetic recording," *Eur. Phys. J. B.*, vol. 86, no. 81, pp. 81, 2013. doi: 10.1140/epjb/e2012-30655-3

⁸ B. Varghese, K. K. M. Cher, J. Hu, T. S. Li, Y. Ding and G. Ju, "Substrate Bias Effects on Magnetic and Structural Properties of L₁₀-FePt Based Recording Media," in *IEEE Trans. Magn.*, vol. 52, no. 7, pp. 1-4, 2016. doi: 10.1109/TMAG.2016.2535292

⁹ M. Ohring, "Discharges, Plasmas, and Ion-Surface Interactions," in *Materials Science of Thin Films: Deposition and Structure*, San Diego, CA, USA: Academic Press, pp. 176, 2002.

¹⁰ G. Betz, "Alloy Sputtering," *Surf. Sci.*, vol. 92, no. 1, pp. 283 – 309, 1980. doi: 10.1016/0039-6028(80)90258-7

¹¹ E. Yang, D. E. Laughlin, and J.-G. Zhu, "Correction of Order Parameter Calculations for FePt Perpendicular Thin Films," *IEEE Trans. Magn.*, vol. 48, no. 1, pp. 7-12, 2012. doi: 10.1109/TMAG.2011.2164547

¹² L. Shen, Z.-M. Yuan, J. Q. Goh, T. Zhou, B. Liu, and Y. P. Feng "The Effect of Introduced Defects on Saturation Magnetization and Magnetic Anisotropy Field of L1₀ FePt," *IEEE Trans. Magn.*, vol 47, no. 10, pp. 2422-2124, 2011. doi: 10.1109/TMAG.2011.2147771

¹³ J. E. Wittig, J. Bentley, and L. F. Allard, "In situ investigation of ordering phase transformations in FePt magnetic nanoparticles," *Ultramicroscopy*, vol. 176, pp. 217-232, 2017. doi: 10.1016/j.ultramic.2016.11.025

¹⁴ A. C. Johnston-Peck, G. Scarel, J. Wang, G. N. Parsons, and J. B. Tracy, "Sinter-free phase conversion and scanning transmission electron microscopy of FePt nanoparticle monolayers," *Nanoscale*, vol. 3, no. 10, pp. 4142-4149, 2011. doi: 10.1039/c1nr10567a